JCARME
ISSN: 2228-7922
Journal of Computational and Applied Research in Mechanical Engineering
Vol. 9, No. 1, pp. 85-101
jcarme.sru.ac.ir

MHD thermal radiation and chemical reaction effects with peristaltic transport of the Eyring-Powell fluid through a porous medium

K. Venugopal Reddy[a, *] and M. Gnaneswara Reddy[b]

[a] *Department of Mathematics, Vignan Institute of Technology & Science, Deshmukhi village, Telangana - 508284, India*

[b] *Department of Mathematics, Acharya Nagarjuna University Campus, Ongole - 523 001, India*

Article info:

Received: 17/08/2017
Accepted: 01/12/2018
Online: 01/12/2018

Keywords:
Peristalsis,
MHD,
Thermal radiation,
Eyring-Powell fluid,
Chemical reaction,
Compliant walls.

Abstract

In this paper, thermal radiation and chemical reaction impacts on MHD peristaltic motion of the Eyring-Powell fluid are analyzed through a porous medium in a channel with compliant walls under slip conditions for velocity, temperature, and concentration. Assumptions of a long wavelength and low Reynolds number are considered. The modeled equations are computed by using the perturbation method. The resulting non-linear system is solved for the stream function, velocity, temperature, concentration, skin-friction coefficient, heat transfer coefficient, and mass transfer coefficient. The flow quantities are examined for various parameters. Temperature is depressed with an enhanced radiation parameter, while the opposite effect is observed for the concentration. The fluid concentration is enhanced and depressed with generative and destructive chemical reaction, respectively. The size of the trapped bolus reduces as the Powel-Eyring parameter increases while it increases as another Powell fluid parameter rises. Furthermore, the size of the trapped bolus grows when Darcy number increases.

Nomenclature

u and v : Velocities
p : Pressure
T : Temperature
C : Concentration
ρ : Density
σ : Electrical conductivity
B_o : Field with Magnetic
c_p : Heat capacity
k : Energy conductivity
D : Mass diffusivity Coefficient
T_m : Mean energy
K_T : Diffusion ratio
k_o : Permeability parameter
k_l : Chemical reaction of the rate constant
σ^* : Boltzmann-Stefan constant
k^* : Absorption mean coefficient
T_0 : Energy at the wall
C_0 : Concentration at the wall
M : Hartmann number
β_1 : Velocity slip

*Corresponding author
email address: venugopal.reddy1982@gmail.com

β_2 : Temperature slip
β_3 : Concentration slip
A and B : Eyring-Powell fluid parameters
θ : Temperature
ϕ : Concentration
Da : Darcy number
Rd : Radiation parameter
γ : Chemical reaction parameter

1. Introduction

The mechanism of the pumping fluid in a channel/tube from a region of minor pressure to major one is known as peristalsis. The peristaltic phenomenon is unique in sensing the that fluid is transported by the action of a progressive sinusoidal wave due to area contraction or expansion, which propagates along an extensible tube/channel instead of using a piston. Peristaltic transporting of non-Newtonian and Newtonian fluids has been extensively recognized by several authors due to its numerous corporeal and engineering applications. In physiology, the peristalsis appears in esophagus over swallowing food, chyme movement in the gastrointestinal tract, urine movement from the kidney to bladder through the ureter, and vasomotion of blood vessels in capillaries and arterioles. The movement of corrosive fluids, sanitary fluid, slurries, and noxious fluids in the nuclear reactor. Furthermore, blood pumps in heart lung machine and roller and finger pumps also function on the principle of peristaltic pumping. The earliest study about the mechanism of peristaltic movement of a viscous fluid was carried out by Latham [1]. Shapiro et al. [2] presented a mathematical model for peristaltic pumping under the assumptions of a creeping flow approximation. He considered the transport of a viscous fluid in a two-dimensional channel. In that study, the authors analyzed the peristaltic pumping reflux and trapping. Afterward, several diagnostic, commutative, and empirical inspections related to peristaltic motions have been studied for different flow geometries and assumptions. Some useful attempts in this direction were described in [3-6]. The analysis in all these attempts has been made by employing no-slip boundary conditions and one or more reduced assumptions of a low Reynolds number, small wave number, long wavelength, etc.

In many research fields, non-Newtonian fluids are considerably used in many corporeal and mechanical processes than Newtonian fluids. Consequently, the Powell-Eyring fluid exemplary is better than the fluid of power law in different ways. Its non-linear equations are proved from the kinetic theory of fluids rather than the experimental relations. Different researchers are analyzed the above statement [7-10]. Recently, few attempts have been investigated in the peristaltic information to analyze the combined impacts of energy and concentration transfer under different situations [11-14].

Radiation heat transfer plays a significant role in the cooling of electronics as well as conduction and convection heat transfer. Thermal radiation has bounteous applications such as freezing, heating, burners, reeking, and solar radiation systems. However, only a few researchers [15-18] have studied radiation in mechanism of peristalsis.

The aim of the current study is to analyze the impacts of thermal and synthetic reactions on MHD peristaltic flow of the Eyring-Powell fluid through a porous medium with wall properties. A mathematical model of the flow and heat and mass transfer, for the present problem, is constructed with imposing long wavelength and low Reynolds number approximations. Series solutions are matured for a small fluid parameter by a regular perturbation procedure. Numerical results for the emerging non-dimensional parameters on different parameters of interest are shown graphically and analyzed. Also, the trapping approach is presented for the pertinent parameters.

2. Modeling

The peristaltic motion of a viscous electrically conducting, radiating and reacting motion of Powell - Eyring

incompressible fluid filled with a porous medium in a two-dimensional channel of width $2d_1$ is considered. The movement of the existing problem with geometry is conferred in Fig. 1.

The physical interpretation of the wall surface is given by:

$$y = \pm\eta(x,t) = \pm\left[d_1 + a\sin\frac{2\pi}{\lambda}(x - ct) \right] \quad (1)$$

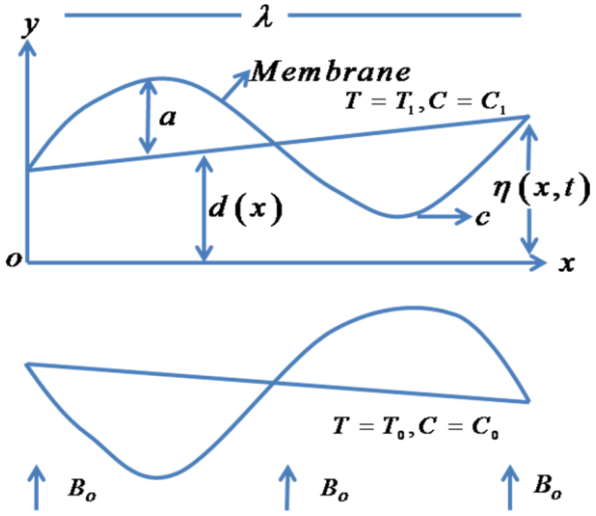

Fig.1. Flow configuration

The Powell-Eyring fluid exemplary is examined to investigate the non-Newtonian motion with shear. The Powell-Eyring fluid model with stress tensor is [13-18]:

$$\boldsymbol{\tau} = \left[\mu + \frac{1}{\beta_{\dot\gamma}} S\sinh^{-1}\left(\frac{1}{c_1}\dot\gamma\right) \right]\mathbf{A}_1 \quad (2)$$

where

$$\dot\gamma = \sqrt{\frac{1}{2}tr(\mathbf{A}_1)^2}\ ,\ \mathbf{A}_1 = (grad\,\mathbf{V})^T + grad\,\mathbf{V}$$

the $S\sinh^{-1}$ up as terms order of second is developed as:

$$S\sinh^{-1}\left(\frac{1}{c_1}\dot\gamma\right) \cong \frac{\dot\gamma}{c_1} - \frac{\dot\gamma^3}{6c_1^3}, \frac{\dot\gamma^5}{c_1^5} << 1 \quad (3)$$

The fundamental equations are [15-18]:

$$\frac{\partial v}{\partial y} + \frac{\partial u}{\partial x} = 0 \quad (4)$$

$$\rho\left(u\frac{\partial u}{\partial x} + v\frac{\partial u}{\partial y} + \frac{\partial u}{\partial t}\right) = -\frac{\partial p}{\partial x} + \left(\mu + \frac{1}{\beta c_1}\right)\left(\frac{\partial^2 u}{\partial x^2} + \frac{\partial^2 u}{\partial y^2}\right) - \sigma B_0^2 u - \frac{\mu}{k_0}u$$
$$-\frac{1}{3\beta c_1^3}\frac{\partial}{\partial x}\left[\frac{\partial u}{\partial x}\left\{2\left(\frac{\partial u}{\partial x}\right)^2 + \left(\frac{\partial u}{\partial y} + \frac{\partial v}{\partial x}\right)^2 + 2\left(\frac{\partial v}{\partial y}\right)^2\right\}\right]$$
$$-\frac{1}{6\beta c_1^3}\frac{\partial}{\partial y}\left[\left(\frac{\partial u}{\partial y} + \frac{\partial v}{\partial x}\right)\left\{2\left(\frac{\partial u}{\partial x}\right)^2 + \left(\frac{\partial u}{\partial y} + \frac{\partial v}{\partial x}\right)^2 + 2\left(\frac{\partial v}{\partial y}\right)^2\right\}\right] \quad (5)$$

$$\rho\left(\frac{\partial v}{\partial t} + u\frac{\partial v}{\partial x} + v\frac{\partial v}{\partial y}\right) = -\frac{\partial p}{\partial y} + \left(\mu + \frac{1}{\beta c_1}\right)\left(\frac{\partial^2 v}{\partial x^2} + \frac{\partial^2 v}{\partial y^2}\right) - \frac{\mu}{k_0}v$$
$$-\frac{1}{6\beta c_1^3}\frac{\partial}{\partial x}\left[\left(\frac{\partial u}{\partial y} + \frac{\partial v}{\partial x}\right)\left\{2\left(\frac{\partial u}{\partial x}\right)^2 + \left(\frac{\partial u}{\partial y} + \frac{\partial v}{\partial x}\right)^2 + 2\left(\frac{\partial v}{\partial y}\right)^2\right\}\right]$$
$$-\frac{1}{3\beta c_1^3}\frac{\partial}{\partial y}\left[\frac{\partial v}{\partial y}\left\{2\left(\frac{\partial u}{\partial x}\right)^2 + \left(\frac{\partial u}{\partial y} + \frac{\partial v}{\partial x}\right)^2 + 2\left(\frac{\partial v}{\partial y}\right)^2\right\}\right] \quad (6)$$

$$\rho C_p\left(u\frac{\partial T}{\partial x} + v\frac{\partial T}{\partial y} + \frac{\partial T}{\partial t}\right) = k\left(\frac{\partial^2 T}{\partial y^2} + \frac{\partial^2 T}{\partial x^2}\right) + \left(\mu + \frac{1}{\beta c_1}\right)\left[4\left(\frac{\partial u}{\partial x}\right)^2 + \left(\frac{\partial u}{\partial y} + \frac{\partial v}{\partial x}\right)^2\right]$$
$$-\frac{2}{3\beta c_1^3}\left(\frac{\partial u}{\partial x}\right)^2\left[\left\{2\left(\frac{\partial u}{\partial x}\right)^2 + 2\left(\frac{\partial v}{\partial y}\right)^2\right\} + \left(\frac{\partial u}{\partial y} + \frac{\partial v}{\partial x}\right)^2\right]$$
$$-\frac{1}{6\beta c_1^3}\left(\frac{\partial u}{\partial y} + \frac{\partial v}{\partial x}\right)^2\left[\left\{2\left(\frac{\partial u}{\partial x}\right)^2 + \left(\frac{\partial u}{\partial y} + \frac{\partial v}{\partial x}\right)^2\right\} + 2\left(\frac{\partial v}{\partial y}\right)^2\right] - \frac{\partial q_r}{\partial y} \quad (7)$$

$$u\frac{\partial C}{\partial x} + v\frac{\partial C}{\partial y} + \frac{\partial C}{\partial t} = D\left(\frac{\partial^2 C}{\partial x^2} + \frac{\partial^2 C}{\partial y^2}\right) + \frac{DK_T}{T_m}\left(\frac{\partial^2 T}{\partial x^2} + \frac{\partial^2 T}{\partial y^2}\right) - k_l(C - C_o) \quad (8)$$

The heat flow of radiation in the direction of $X-$axis is studied as negligible compared to

the $Y-$axis. The heat flow of the radiation q_r is defined using the approximation of the Rosseland for thermic radiation as given by:

$$q_r = -\frac{16\sigma^* T_o^3}{3k^*}\frac{\partial T}{\partial Y} \tag{9}$$

The associated boundary conditions are:

$$\frac{\partial}{\partial x}\left(-\tau\frac{\partial^2}{\partial x^2}+m\frac{\partial^2}{\partial t^2}+d\frac{\partial}{\partial t}\right)\eta=\left(\mu+\frac{1}{\beta c_1}\right)\left(\frac{\partial^2 u}{\partial x^2}+\frac{\partial^2 u}{\partial y^2}\right)-\sigma B_o^2 u-\frac{\mu}{k_o}u-\rho\left(u\frac{\partial u}{\partial x}+v\frac{\partial u}{\partial y}+\frac{\partial u}{\partial t}\right)-\frac{1}{6\beta c_1^3}\frac{\partial}{\partial y}\left[\left(\frac{\partial u}{\partial y}+\frac{\partial v}{\partial x}\right)\left\{\begin{matrix}2\left(\frac{\partial u}{\partial x}\right)^2+2\left(\frac{\partial v}{\partial y}\right)^2\\+\left(\frac{\partial u}{\partial y}+\frac{\partial v}{\partial x}\right)^2\end{matrix}\right\}\right]-\frac{1}{3\beta c_1^3}\frac{\partial}{\partial x}\left[\frac{\partial u}{\partial x}\left\{\begin{matrix}2\left(\frac{\partial u}{\partial x}\right)^2+\left(\frac{\partial u}{\partial y}+\frac{\partial v}{\partial x}\right)^2\\+2\left(\frac{\partial v}{\partial y}\right)^2\end{matrix}\right\}\right] \quad \text{at } y=\pm\eta \tag{10}$$

$$u\pm\beta_1\left(\frac{\partial u}{\partial y}+\frac{\partial v}{\partial x}\right)\left[\left(\mu+\frac{1}{\beta c_1}\right)-\frac{\mu}{k_0}v-\frac{1}{6\beta c_1^3}\left\{\begin{matrix}2\left(\frac{\partial u}{\partial x}\right)^2+2\left(\frac{\partial v}{\partial y}\right)^2\\+\left(\frac{\partial u}{\partial y}+\frac{\partial v}{\partial x}\right)^2\end{matrix}\right\}\right]=0 \quad \text{at } y=\pm\eta \tag{11}$$

$$T\pm\beta_2\frac{\partial T}{\partial y}=T_0,\ C\pm\beta_3\frac{\partial C}{\partial y}=C_0$$

at $y=\pm\eta$ (12)

Proposing the stream function $\psi(x,y,t)$

$$v=-\frac{\partial\psi}{\partial x}, u=\frac{\partial\psi}{\partial y} \tag{13}$$

and defining dimensionless quantities of:

$$x^*=\frac{x}{\lambda},\ y^*=\frac{y}{d_1},\ \psi^*=\frac{\psi}{cd_1},\ t^*=\frac{ct}{\lambda},\ \eta^*=\frac{\eta}{d_1},$$
$$p^*=\frac{pd_1^2}{c\lambda\mu},\ B=\frac{1}{\mu\beta c_1}, A=\frac{Bc^2}{2d_1^2c_1^2},\ \delta=\frac{d_1}{\lambda}, \theta=\frac{T-T_o}{T_o},$$
$$\varphi=\frac{C-C_o}{C_o},\ \mathrm{Re}=\frac{\rho c d_1}{\mu},\ M=\sqrt{\frac{\sigma}{\mu}}B_o d_1, E_1=\frac{-\tau d_1^3}{\lambda^3\mu c},$$
$$E_2=\frac{mcd_1^3}{\lambda^3\mu},\ E_3=\frac{dd_1^3}{\lambda^2\mu}, \beta_i^*=\frac{\beta_i}{d_i}(i=1-3),$$
$$\mathrm{Pr}=\frac{\mu c_p}{k},\ Ec=\frac{c^2}{C_pT_o},\ Sc=\frac{\mu}{D\rho},\ Sr=\frac{\rho DK_TT_o}{\mu T_mC_o},$$
$$\gamma=k_l\frac{d_1^2}{\nu},\ Da=\frac{k_o}{d_1^2}, Rd=\frac{16\sigma^*T_o^3}{3k^*\bar{\mu}_o c_f},\ Br=\mathrm{Pr}\,Ec \tag{14}$$

Using Eq. (13) and quantities (14) into Eqs. (5-12), and to apply the creeping flow approximations, it is accessed the following non-dimensional equations (after dropping asterisks):

$$(1+B)\frac{\partial^3\psi}{\partial y^3}-\frac{A}{3}\frac{\partial}{\partial y}\left(\frac{\partial^2\psi}{\partial y^2}\right)^3-\left(M^2+\frac{1}{Da}\right)\frac{\partial\psi}{\partial y}=\frac{\partial p}{\partial x} \tag{15}$$

$$\frac{\partial p}{\partial y}=0 \tag{16}$$

$$\left(\frac{1}{\mathrm{Pr}}+Rd\right)\frac{\partial^2\theta}{\partial y^2}+Ec\left(\frac{\partial^2\psi}{\partial y^2}\right)^2\left[(1+B)-\frac{A}{3}\left(\frac{\partial^2\psi}{\partial y^2}\right)^2\right]=0 \tag{17}$$

$$\frac{\partial^2\phi}{\partial y^2}+ScSr\frac{\partial^2\theta}{\partial y^2}-Sc\gamma\phi=0 \tag{18}$$

The corresponding boundary conditions are:

$$\frac{\partial}{\partial x}\left(E_1\frac{\partial^2}{\partial x^2}+E_2\frac{\partial^2}{\partial t^2}+E_3\frac{\partial}{\partial t}\right)\eta=(1+B)\frac{\partial^3\psi}{\partial y^3}-\frac{A}{3}\frac{\partial}{\partial y}\left(\frac{\partial^2\psi}{\partial y^2}\right)^3-\left(M^2+\frac{1}{Da}\right)\frac{\partial\psi}{\partial y} \quad \text{at } y=\pm\eta \tag{19}$$

$$\frac{\partial \psi}{\partial y} \pm \beta_1 \left[(1+B)\frac{\partial^2 \psi}{\partial y^2} - \frac{A}{3}\left(\frac{\partial^2 \psi}{\partial y^2}\right)^3 \right] = 0,$$

$$\theta \pm \beta_2 \frac{\partial \theta}{\partial y} = 0\,, \phi \pm \beta_3 \frac{\partial \phi}{\partial y} = 0 \qquad (20)$$

Eliminating pressure by cross differentiation from Eqs. (15 and 16):

$$(1+B)\frac{\partial^4 \psi}{\partial y^4} - \frac{A}{3}\frac{\partial^2}{\partial y^2}\left(\frac{\partial^2 \psi}{\partial y^2}\right)^3 - \left(M^2 + \frac{1}{Da}\right)\frac{\partial^2 \psi}{\partial y^2} = 0 \qquad (21)$$

3. Perturbation solution

The non-dimensional governing Eqs. (21, 17 and 18) are coupled, and extremely non-linear and their exact solutions may not be possible. Therefore, in order to obtain approximate series solutions, expressions for ψ, θ and ϕ in small Eyring-Powell fluid parameter A are expanded as follows:

$$\begin{aligned} \psi &= A\psi_1 + \psi_o + O\left(A^2\right), \\ \theta &= A\theta_1 + \theta_o + O\left(A^2\right), \\ \varphi &= A\varphi_1 + \varphi_o + O\left(A^2\right). \end{aligned} \qquad (22)$$

Substituting Eq. (22) into Eqs. (21, 17 and 18) and the associated boundary conditions (19) and (20), the following systems of zeroth (Section 3.1) and first order (Section 3.2) are taken:

3.1. Zeroth order system

$$(1+B)\frac{\partial^4 \psi_o}{\partial y^4} - \left(M^2 + \frac{1}{Da}\right)\frac{\partial^2 \psi_o}{\partial y^2} = 0 \qquad (23)$$

$$\left(\frac{1}{\Pr} + Rd\right)\frac{\partial^2 \theta_o}{\partial y^2} + Ec(1+B)\left(\frac{\partial^2 \psi_o}{\partial y^2}\right)^2 = 0 \qquad (24)$$

$$\frac{\partial^4 \phi_o}{\partial y^4} + ScSr\frac{\partial^2 \theta_o}{\partial y^2} - Sc\gamma\phi_o = 0 \qquad (25)$$

and the corresponding boundary conditions are:

$$\frac{\partial}{\partial x}\left(E_2\frac{\partial^2}{\partial t^2} + E_1\frac{\partial^2}{\partial x^2} + E_3\frac{\partial}{\partial t}\right)\eta = (1+B)\frac{\partial^3 \psi_o}{\partial y^3} - \left(M^2 + \frac{1}{Da}\right)\frac{\partial \psi_o}{\partial y}$$

, at $y = \pm\eta$ (26)

$$\frac{\partial \psi_o}{\partial y} \pm \beta_1(1+B)\frac{\partial^2 \psi_o}{\partial y^2} = 0\,, \beta_2\frac{\partial \theta_o}{\partial y} \pm \theta_o = 0\,,$$

$$\beta_3\frac{\partial \varphi_o}{\partial y} \pm \varphi_o = 0 \text{ at } y = \pm\eta \qquad (27)$$

Solving the Eqs. (23, 24) and 25) with corresponding boundary conditions (26) and (27), the solutions are obtained as follows:

$$\psi_o = L_2 \sinh(Ny) + L_3 y \qquad (28)$$

$$\theta_o = B_1 + B_2 y + L_{10}\cosh(2Ny) + L_{11}y^2 \qquad (29)$$

$$\varphi_o = C_1\cosh(N_2 y) + C_2\sinh(N_2 y) + L_{25}\cosh(2Ny) + L_{26} \qquad (30)$$

3.2. First order system

$$(1+B)\frac{\partial^4 \psi_1}{\partial y^4} - \frac{1}{3}\frac{\partial^2}{\partial y^2}\left(\frac{\partial^2 \psi_o}{\partial y^2}\right)^3 - \left(M^2 + \frac{1}{Da}\right)\frac{\partial^2 \psi_1}{\partial y^2} = 0 \qquad (31)$$

$$\left(\frac{1}{\Pr} + Rd\right)\frac{\partial^2 \theta_1}{\partial y^2} + 2Ec(1+B)\left(\frac{\partial^2 \psi_o}{\partial y^2}\frac{\partial^2 \psi_1}{\partial y^2}\right) - \frac{1}{3}Ec\left(\frac{\partial^2 \psi_o}{\partial y^2}\right)^4 = 0 \qquad (32)$$

$$\frac{\partial^2 \phi_1}{\partial y^2} + ScSr\frac{\partial^2 \theta_1}{\partial y^2} - Sc\gamma\phi_1 = 0 \qquad (33)$$

and the boundary conditions associated with the above equations are:

$$(1+B)\frac{\partial^3\psi_1}{\partial y^3}-\frac{1}{3}\frac{\partial}{\partial y}\left(\frac{\partial^2\psi_o}{\partial y^2}\right)^3-\left(M^2+\frac{1}{Da}\right)\frac{\partial\psi_1}{\partial y}=0$$
at $y=\pm\eta$ (34)

$$\frac{\partial\psi_1}{\partial y}\pm\beta_1\left[(1+B)\frac{\partial^2\psi_1}{\partial y^2}-\frac{1}{3}\left(\frac{\partial^2\psi_o}{\partial y^2}\right)^3\right]=0,$$
$$\theta_1\pm\beta_2\frac{\partial\theta_1}{\partial y}=0,\ \phi_1\pm\beta_3\frac{\partial\phi_1}{\partial y}=0 \text{ at } y=\pm\eta$$
(35)

Now using the solutions obtained at the zeroth order system into the first order system and then solving the resulting problem, the followings are finally attained:

$$\psi_1=L_8\sinh(Ny)+L_6\sinh(3Ny)+L_7y\cosh(Ny)$$ (36)

$$\theta_1=B_3+B_4y+L_{14}\sinh(2Ny)+L_{20}\cosh(2Ny)+L_{21}\cosh(4Ny)+L_{22}y\sinh(2Ny)+L_{23}y^2$$ (37)

$$\varphi_1=C_4\sinh(N_2y)+C_3\cosh(N_2y)+L_{28}\sinh(2Ny)+L_{29}\cosh(2Ny)+L_{30}\cosh(4Ny)+L_{31}y\sinh(2Ny)+L_{32}$$ (38)

where the constants are convoluted in Eqs. (28-30) and Eqs. (36-38) are defined in the Appendix.

4. Results and discussions

This section aims to analyze the obtained results graphically. The variations in velocity, energy, mass particle, stream lines, heat and mass transfer coefficients caused by different physical parameters on the quantities of interest are discussed through Figs. 2-44. The following default fixed constants are adopted for numerical computation:

$E_1=0.4,\ E_2=0.1,\ E_3=0.01,\ \varepsilon=0.15,\ x=0.2,$
$B=2, M=1.0,\ \beta_1=0.01,\ A=0.1,\ Da=0.3,$
$t=0.1,\ Br=2, \beta_2=0.02,\ \Pr=1,\ Rd=1,$
$Sc=1,\ \gamma=1, Sr=1, \beta_3=0.02,\ x=0.2$

4.1. Flow characteristics

This section provides the variation of different physical parameters of interest on the axial velocity u, which is obtained using the expression $u=\frac{\partial\psi_o}{\partial y}+A\frac{\partial\psi_1}{\partial y}$. Fig. 2 shows that the axial velocity enhances as the effect of material parameter A increases. it involves the governing non-linear momentum while axial velocity retards with the rise in other material parameter B given in Fig. 3. Fig. 4 represents that with the rise of Hartmann number M the axial velocity is retarded. . It is because of the Lorentz force combined with the applied magnetic field along the transverse direction which resists against the flow. Fig. 5 depicts that the axial velocity enhances by increasing slip parameter β_1 while the quite opposite behavior is observed on the axial velocity when a rise in Darcy number Da happens. This is because it leads to reduce the drag force and consequently the flow velocity increases as Fig. 6 demonstrates. Fig. 7 notices that the axial velocity rises with enhancing E_1 or E_2, while the axial velocity diminishes by increasing wall damping parameter E_3.

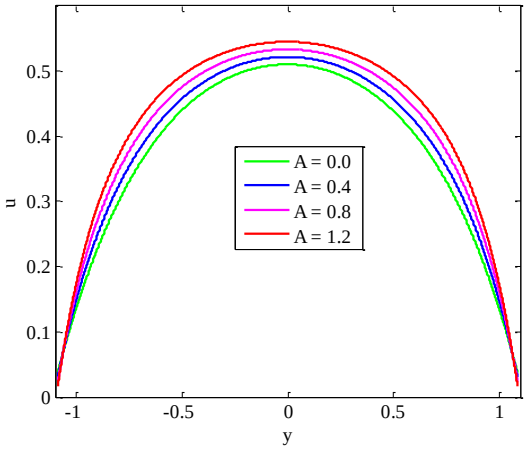

Fig. 2. u response for A.

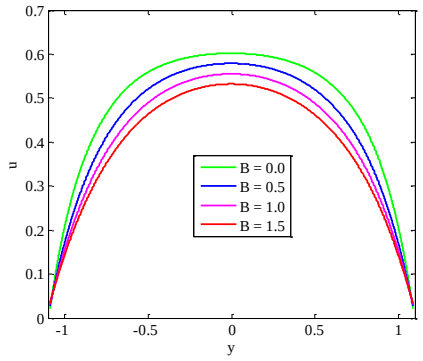

Fig. 3. u response for B.

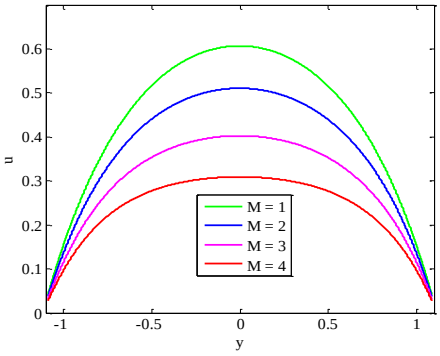

Fig. 4. u response for M.

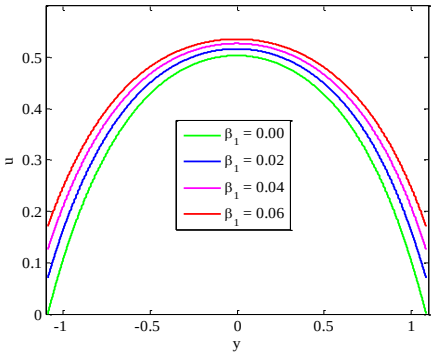

Fig. 5. u response for β_1.

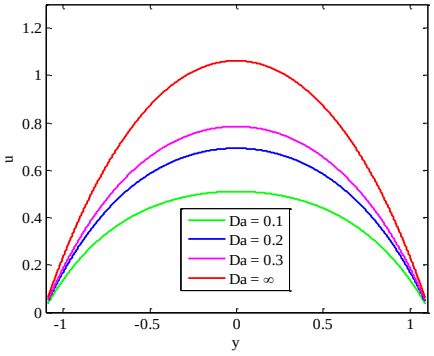

Fig. 6. u response for Da.

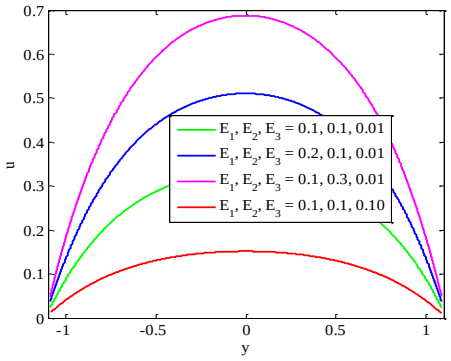

Fig. 7. u response for E_1, E_2 *and* E_3.

4.2. Heat characteristics

Here, the impact of different physical parameters of interest on the temperature distribution (θ), which is obtained using the expression $\theta = \theta_0 + A\theta_1$ from Figs. 8 – 17, is investigated. It is found that in these figures the temperature is greater at the middlemost of the channel compared to the walls. This is due to the fact that the study of dissipation impacts on the temperature. The temperature increases by increasing Powell-Eyring fluid parameter A as shown in Fig. 8, while it has opposite behavior in the magnitude of another Eyring-Powell fluid parameter B (Fig. 9). The energy diminishes with an increase in M, β_1, $\Pr$, Da and Rd as shown in Figs. 10 – 14, while the quite opposite trend is observed with an increase of thermal slip parameter β_2 and Brinkman number Br, based on Figs. 15 – 16. Fig. 17 illustrates that the energy enhances with an increase in E_1 and E_2, while it depresses with an increase in E_3.

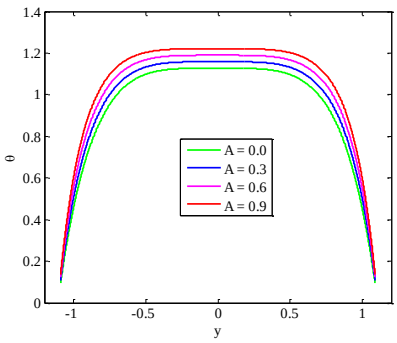

Fig. 8. θ response for A.

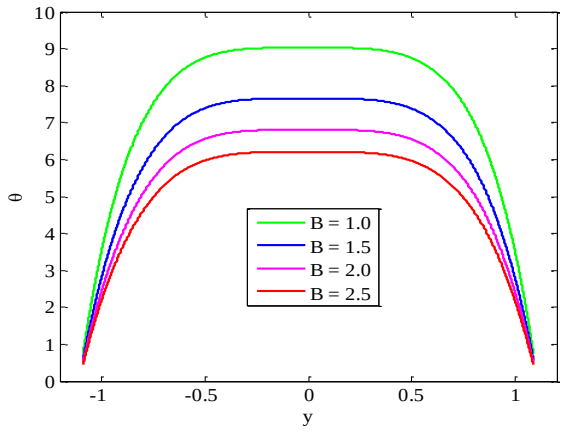

Fig. 9. θ response for B.

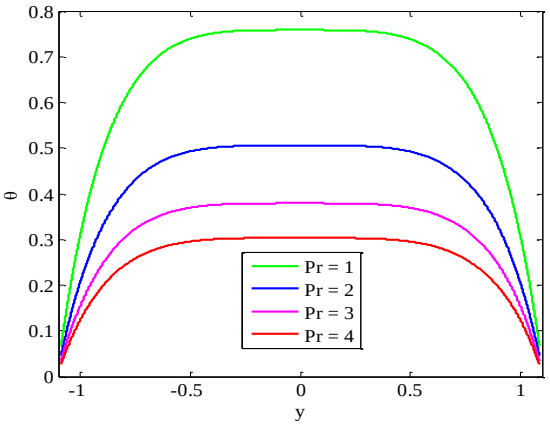

Fig. 12. θ response for $\Pr$.

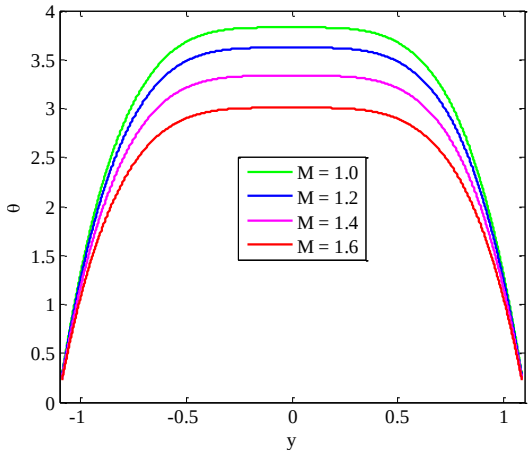

Fig. 10. θ response for M.

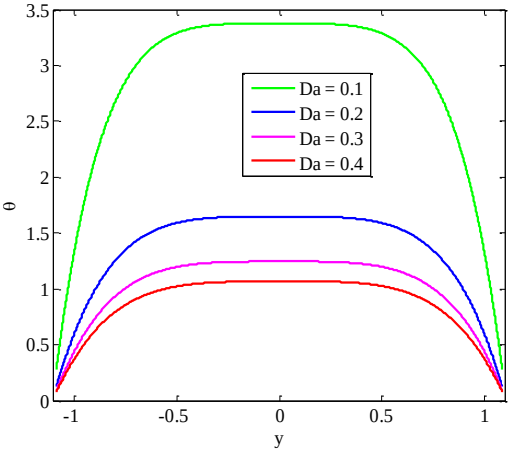

Fig. 13. θ response for Da.

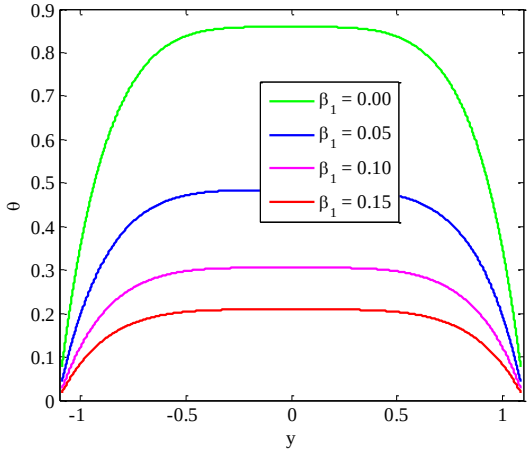

Fig. 11. θ response for β_1.

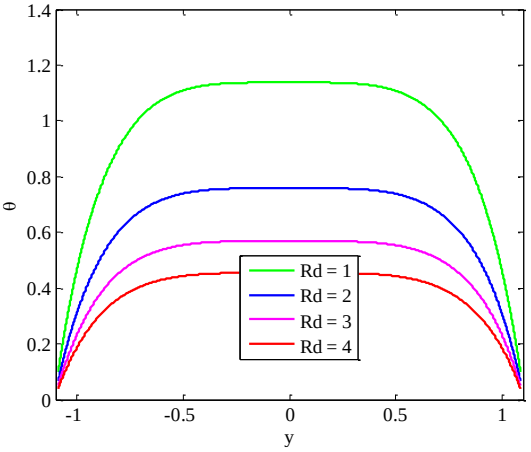

Fig. 14. θ response for Rd.

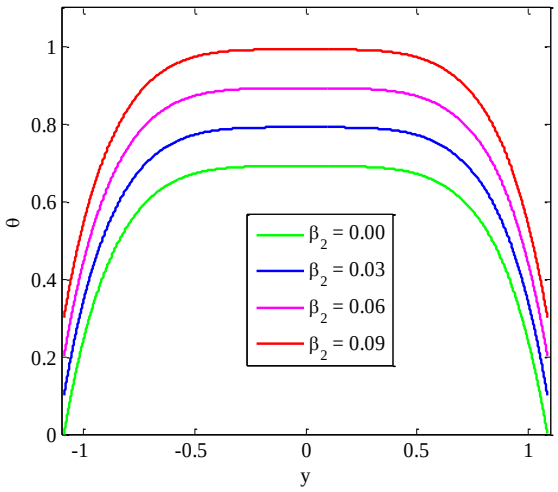

Fig. 15. θ response for β_2.

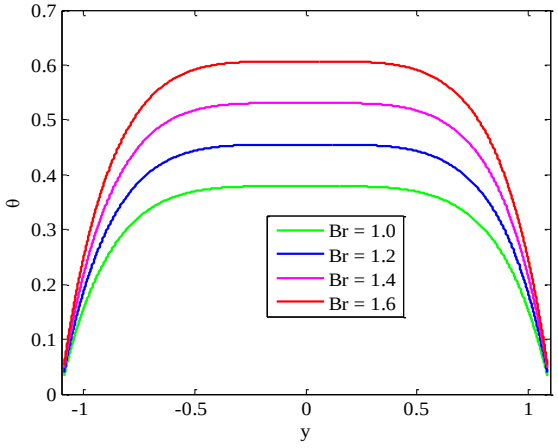

Fig. 16. θ response for Br.

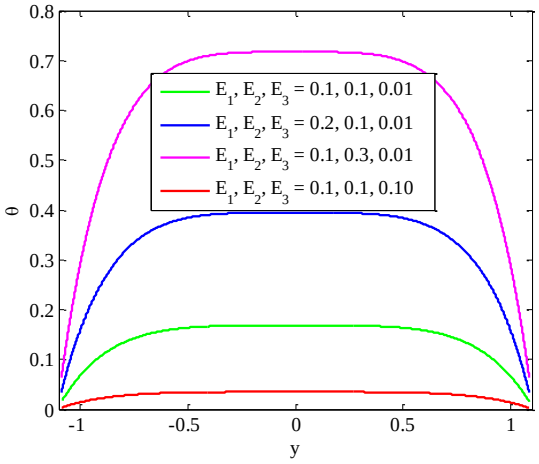

Fig. 17. θ response for E_1, E_2 *and* E_3.

4.3. Mass characteristics

In this section, it is found that the effect of various parameters of interest on the mass distribution (ϕ) which is computed using the expression $\phi = \phi_0 + A\phi_1$ through Figs. 18 - 27. The Figs. 18 - 19 show that the concentration distribution depresses as the larger values of Eyring – Powell parameter A from Fig. 18 while Fig. 19 exhibits opposite behavior as the higher values of another Eyring – Powell parameter B. The concentration distribution enhances with the effect of the higher values of Hartmann number M as well as Da ,as shown in Figs. 20 and 21, while the concentration has opposite behavior with an increase in concentration slip parameter β_3, Brinkman number Br, and Schmidt number Sc, as illustrated in Figs. 22 - 24. Fig. 25 shows that the concentration increases with the rise in the value of the radiation parameter Rd while it follows the same behavior with the increase in chemical reaction parameter γ (Fig. 26). Fig. 27 depicts that the energy depresses with an enhance in E_1 and E_2, while it intensifies with an increase in E_3.

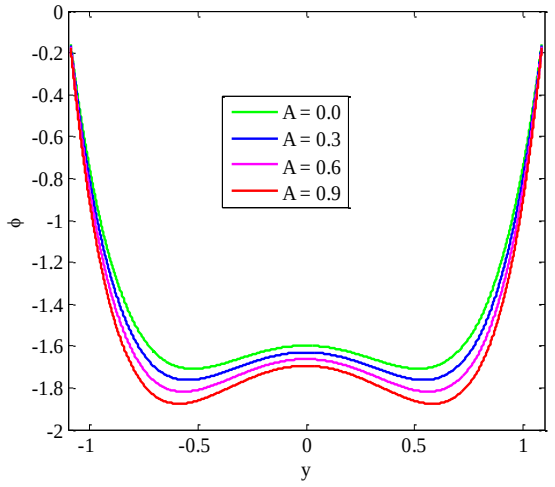

Fig. 18. ϕ response for A.

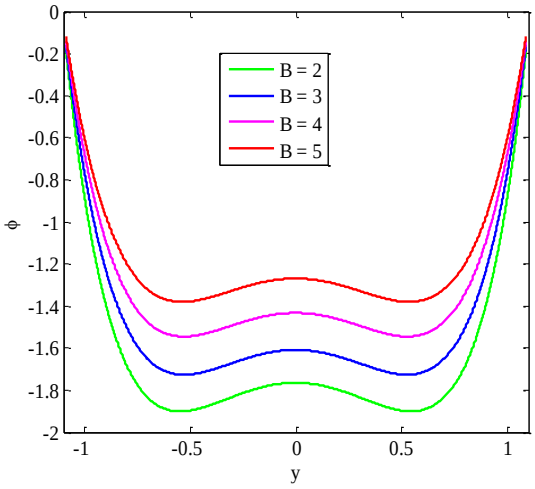

Fig. 19. ϕ response for B.

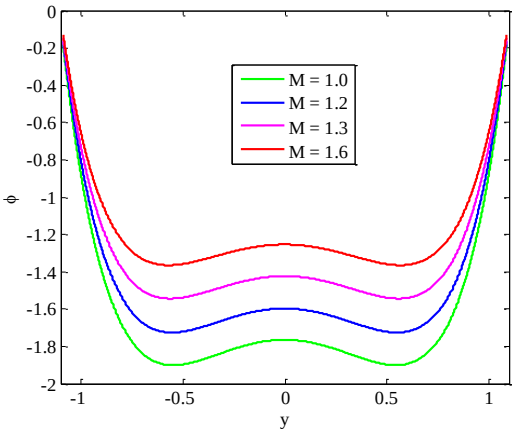

Fig. 20. ϕ response for M.

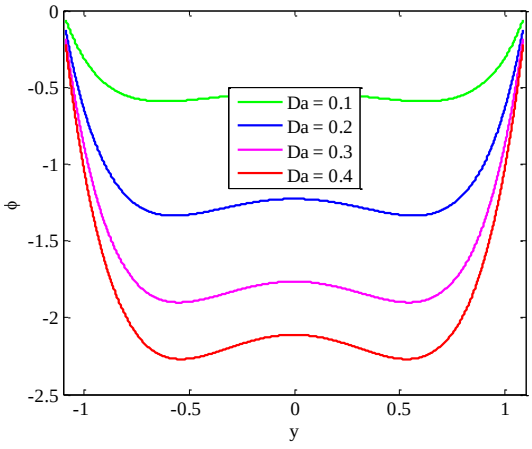

Fig. 21. ϕ response for Da.

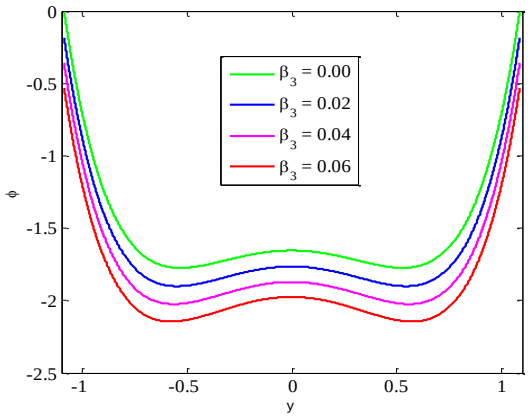

Fig. 22. ϕ response for β_3.

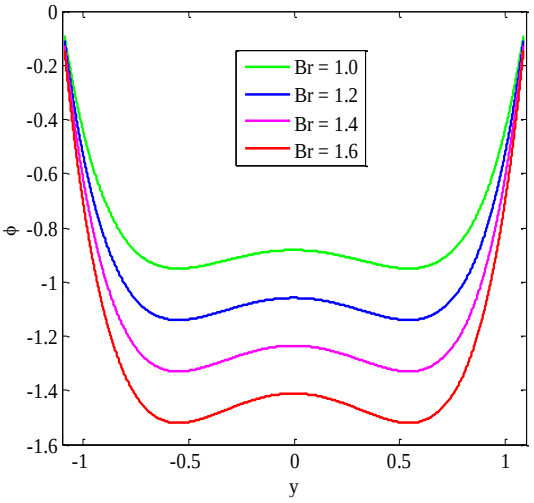

Fig. 23. ϕ response for Br.

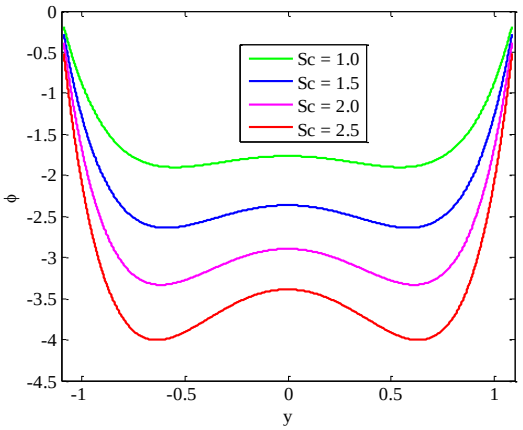

Fig. 24. ϕ response for Sc.

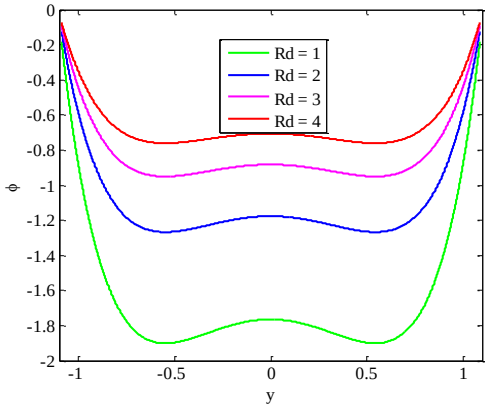

Fig. 25. ϕ response for Rd .

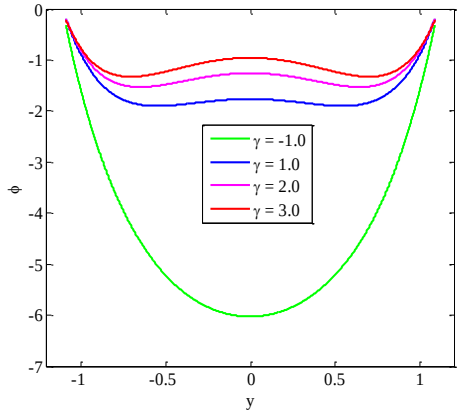

Fig. 26. ϕ response for γ .

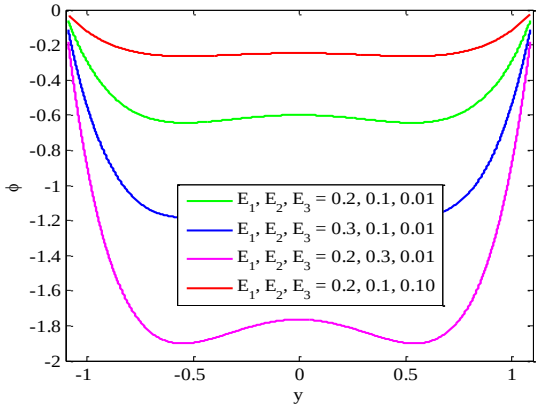

Fig. 27. ϕ response for $E_1, E_2 \; and \; E_3$.

4.4. Skin – friction coefficient

Here, the impact of different parameters of interest on c_f , which is simplified using the following expression, is achieved.

$$c_f = \eta_x \psi_{yy}(\eta) = \eta_x \left[\psi_{0yy}(\eta) + A\psi_{1yy}(\eta) \right].$$

Figs. 28 and 29 provide that the absolute value of skin - friction coefficient enhances with an increase in Hartmann number M and Darcy number Da .

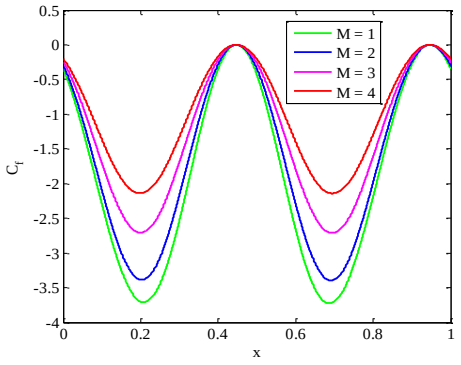

Fig. 28. C_f response for M .

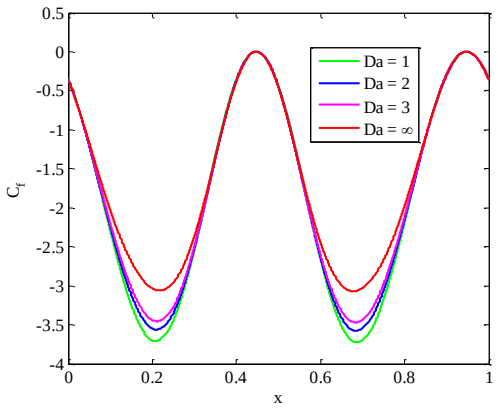

Fig. 29. C_f response for Da .

4.5. Nusselt number

Here, as Fig. 30-35 propose, the impact of different parameters of interest on Nusselt number Nu , which is evaluated using the following expression, is obtained. $Nu = \eta_x \theta_y(\eta) = \eta_x \left[\theta_{0y}(\eta) + A\theta_{1y}(\eta) \right]$ The Nusselt number Nu rises at the minor wall followed by diminishing at the major wall with the increase in A, Hartmann number M , velocity slip parameter β_1 and Rd as shown in Figs. 30 - 34, respectively. However, it has an opposite behavior with the effect of parameter Br (Fig. 35).

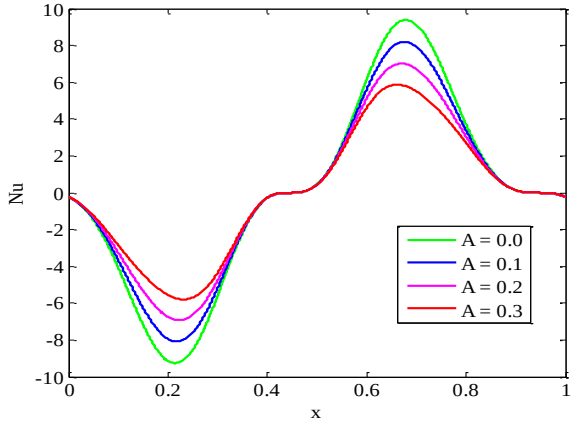

Fig. 30. *Nu* response for A.

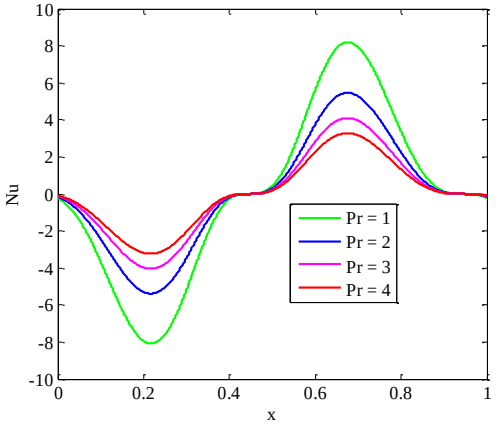

Fig. 33. *Nu* response for Pr.

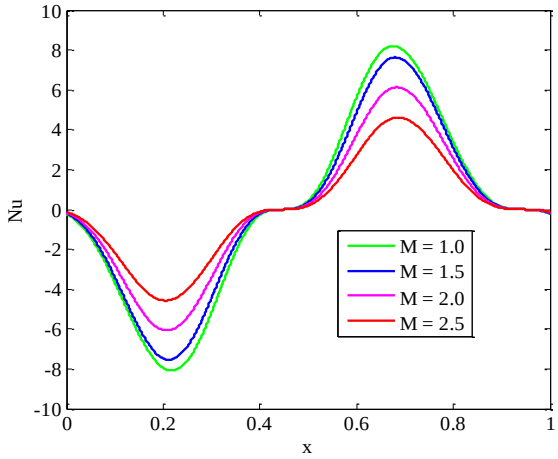

Fig. 31. *Nu* response for M.

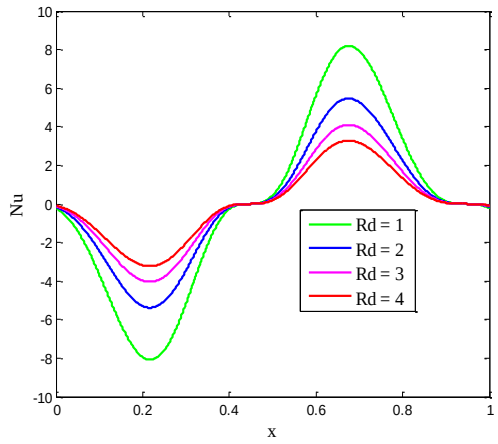

Fig. 34. *Nu* response for Rd.

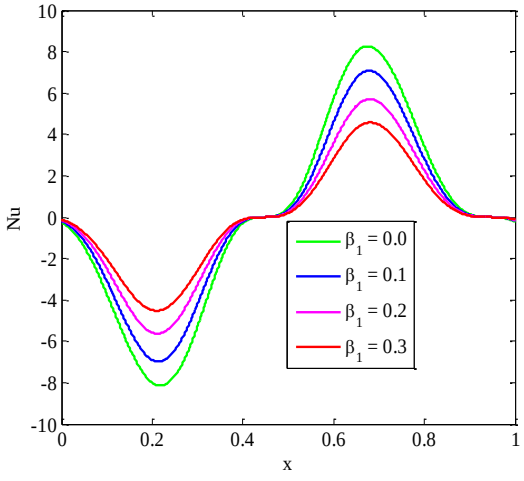

Fig. 32. *Nu* response for β_1.

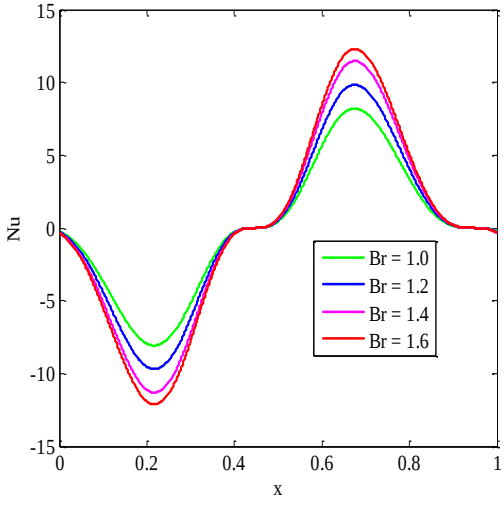

Fig. 35. *Nu* response for Br.

4.6. Sherwood number

Here, the impact of different parameters of interest on Sherwood number Sh, which is simplified using the expression $Sh = \eta_x \phi_y(\eta) = \eta_x \left[\phi_{0y}(\eta) + A\phi_{1y}(\eta)\right]$ is graphically provided in Figs. 36 - 38. It can be inferred that the Sherwood number Sh depresses at the minor wall and enhances at the major wall with increasing the Darcy number Da and chemical reaction parameter γ as shown in Figs. 36 and 37, respectively, while it has an opposite behavior with the effect of radiation parameter , Rd as shown in Fig. 38.

4.7. Trapping phenomenon

Trapping is an important phenomenon in peristaltic motion. In a wave frame, the streamline under particular conditions split to trap a bolus which moves as a whole with the speed of the peristaltic wave. Figs. 39 - 44 show the stream lines for diverse values of adequate parameters of interest. In Figs. 39 - 42, the effect of A on the distribution of velocity is illustrated. In figures 39 and 40, the effect of Eyring-Powell fluid parameter A on the velocity distribution is portrayed. It is observed that the size of the trapped bolus number of circulations increases when Powell fluid parameter A increases. It is also found that size and shape of the boluses are similar in the upper and lower halves of the channel while it has quite opposite behavior for the effect of another Eyring-Powell fluid parameter B increases from Figs. 41-42. Figs. 43 and 44 illustrates that the shape and size of the boluses expand when the Darcy number Da increases.

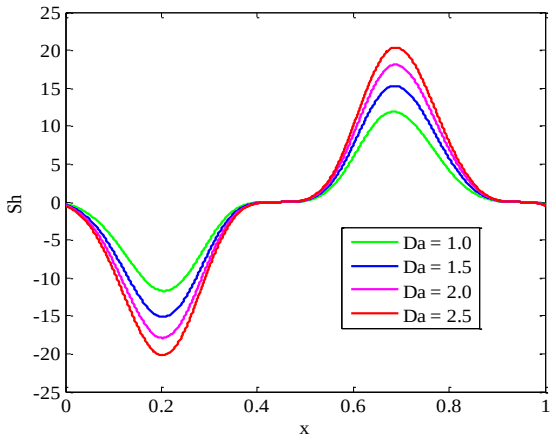

Fig. 36. Sh response for Da.

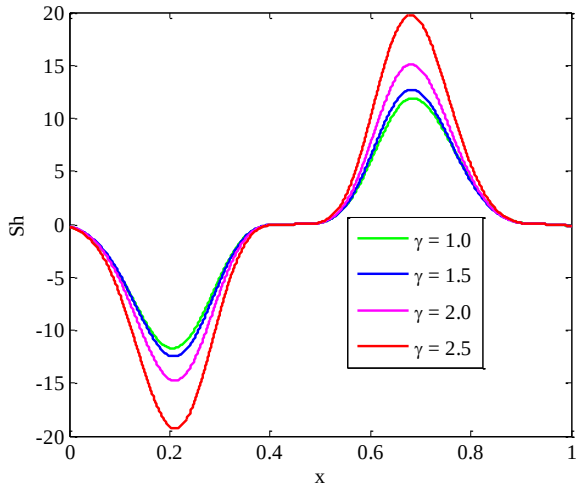

Fig. 37. Sh response for γ.

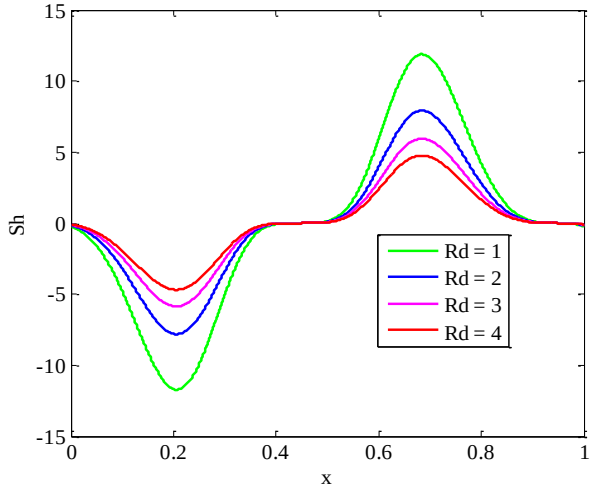

Fig. 38. Sh response for Rd.

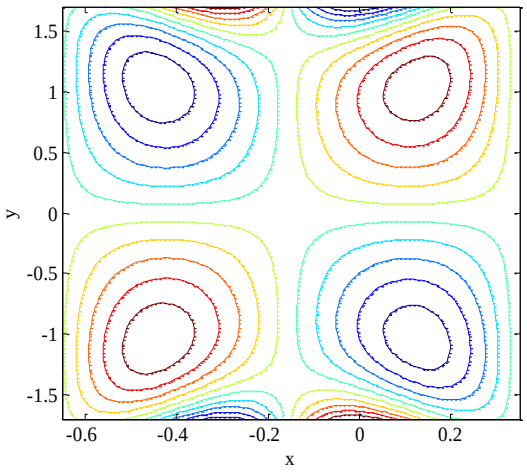

Fig. 39. Stream lines for $A = 0$.

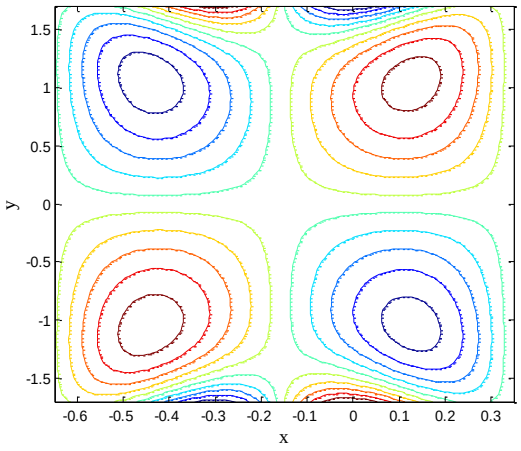

Fig. 40. Stream lines for $A = 3$.

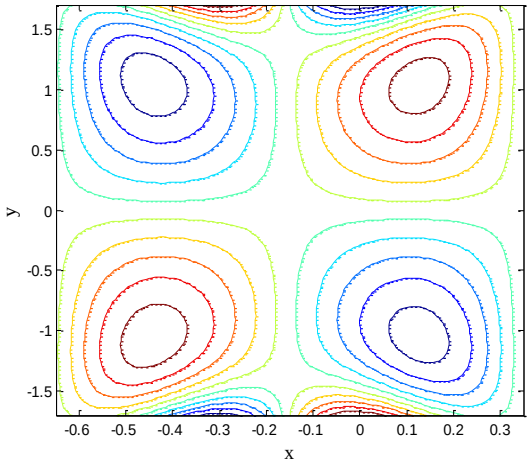

Fig. 41. Stream lines for $B = 1$.

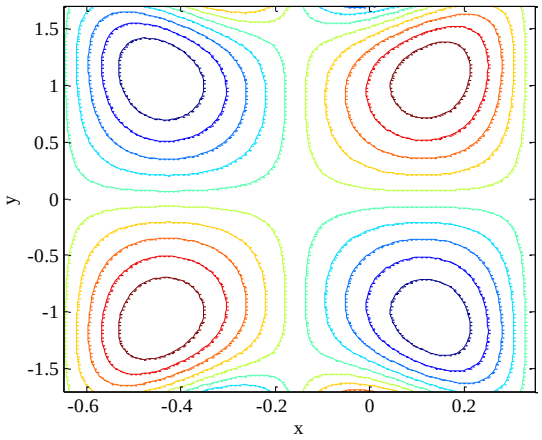

Fig. 42. Stream lines for $B = 3$.

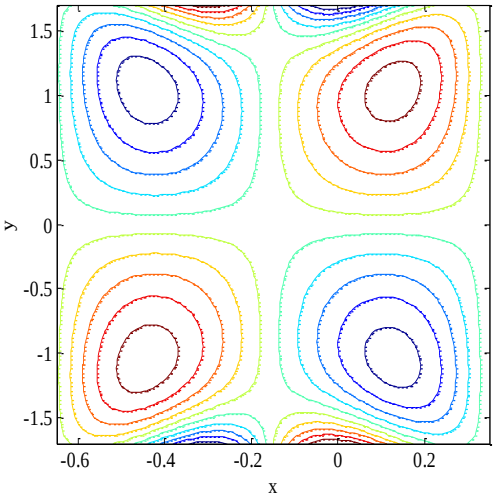

Fig. 43. Stream lines for $Da = 1$.

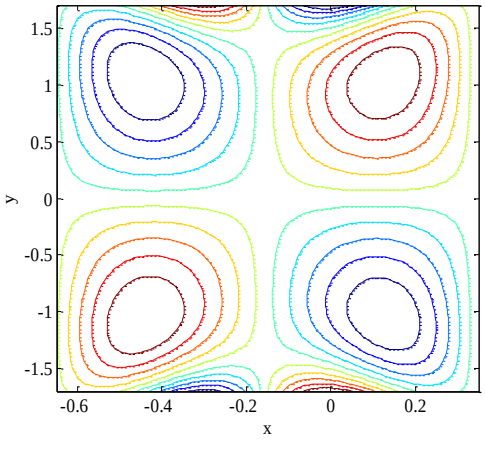

Fig. 44. Stream lines for $Da = \infty$.

5. Conclusions

In the current paper, the MHD motion of chemical reaction and radiation effects on peristaltic flow of Eyring-Powell fluid are analyzed through a porous medium in a complaint wall channel with slip conditions. The governing equations are modeled using Creeping flow approximations, and then the perturbation method is used for the approximate solution of different physical parameters of interest. The significant points of the current analysis are mentioned below:

1. The axial velocity enhances to the higher values of Da.
2. The temperature diminishes with increasing Rd.
3. The concentration increases with the larger values of γ and Rd.
4. If the Darcy number goes to infinity and the absence of chemical reaction parameter, radiation parameter are in good agreement.
5. Nu and Sh are found oscillatory.
6. The size of trapped bolus rises when Da enhances.
7. The size of trapped bolus diminishes as the Powell-Eyring parameter A increases, while it enhances as another Powell fluid parameter B increases.

Appendix

$$N=\sqrt{\frac{\left(M^2+\frac{1}{Da}\right)}{1+B}},$$

$$N_2=\sqrt{Sc\gamma},$$

$$L=\frac{8\pi^3\varepsilon}{(1+B)}\left(\frac{E_3}{2\pi}\sin\left(2\pi(x-t)-(E_1+E_2)\cos\left(2\pi(x-t)\right)\right)\right),$$

$$L_1=\frac{L}{\cosh(N\eta)+\beta_1(1+B)N\sinh(N\eta)},$$

$$L_2=\frac{L_1}{N^3},$$

$$L_3=-\frac{L}{N^2},\ L_4=\frac{3L_2^3N^8}{4(1+B)},\ L_5=-\frac{L_2^3N^8}{4(1+B)},$$

$$L_6=\frac{L_4}{72N^2},\qquad L_7=\frac{L_5}{2N^3},$$

$$L_9=-\frac{\left(Br(1+B)L_2^2N^4\right)}{2(1+\Pr Rd)},\qquad L_{10}=\frac{L_9}{4N^2},$$

$$L_{11}=-\frac{L_9}{2},$$

$$B_1=-L_{10}\cosh(2N\eta)-L_{11}\eta^2-\beta_2\begin{pmatrix}2NL_{10}\sinh(2N\eta)\\+2L_{11}\eta\end{pmatrix}$$

$$B_2=-\frac{1}{\eta+\beta_2}\begin{pmatrix}B_1+L_{10}\cosh(2N\eta)+L_{11}\eta^2\\+\beta_2\left(2NL_{10}\sinh(2N\eta)\right)+2L_{11}\eta\end{pmatrix},$$

$$L_{12}=-\frac{2Br(1+B)}{1+\Pr Rd},\ L_{13}=\frac{Br}{3(1+\Pr Rd)},$$

$$L_{14}=\frac{L_{12}L_2A_7N^2}{8},\ L_{15}=\frac{L_2L_8N^2L_{12}}{8},$$

$$L_{16}=\frac{9L_2N^2L_{12}L_6}{32},\ L_{17}=\frac{L_{12}L_2NL_7}{8},$$

$$L_{18}=\frac{L_2L_7NL_{12}}{4},\ L_{19}=\frac{L_2^4L_7N^8L_{13}}{4},$$

$$L_{20}=L_{15}-4L_{16}-L_{17}+L_{18}-\left(\frac{L_{19}}{2N^2}\right),$$

$$L_{21}=L_{16}+\left(\frac{L_{19}}{32N^2}\right),$$

$$L_{22}=L_{17}N,\ L_{23}=\frac{3}{4}L_{19}-2N^2L_{15}-2N^2L_{18},$$

$$L_{24}=2NL_{20}+L_{22},\ L_{25}=-\frac{4N^2L_{10}ScSr}{4N^2-N_2^2},$$

$$L_{26}=\frac{2ScSrL_{11}}{N_2^2},$$

$$B_4=-\frac{1}{\eta+\beta_2}\begin{pmatrix}L_{14}\sinh(2N\eta)+\\2\beta_2NL_{14}\cosh(2N\eta)\end{pmatrix},$$

$$B_3 = -\left(\begin{array}{l} B_4\eta + L_{14}\sinh(2N\eta) + L_{20}\cosh(2N\eta) + \\ L_{21}\cosh(4N\eta) + L_{22}\eta\sinh(2N\eta) + L_{23}\eta^2 \\ +\beta_2\left(\begin{array}{l} B_4 + 2NL_{14}\cosh(2N\eta) + L_{24}\sinh(2N\eta) \\ +4NL_{21}\sinh(4N\eta) + 2NL_{22}\eta\cosh(2N\eta) \\ +2L_{23}\eta \end{array}\right) \end{array}\right)$$

$$C_2 = 0,$$

$$C_1 = -\frac{1}{\cosh(N_2\eta) + \beta_3 N_2\sinh(N_2\eta)}\left(\begin{array}{l} L_{25}\cosh(2N\eta) + L_{26} + \\ 2NL_{25}\beta_3\sinh(2N\eta) \end{array}\right)$$

,

$$L_{27} = 2NL_{24} + 2NL_{22}, L_{28} = -\frac{4ScSrN^2L_{14}}{4N^2 - N_2^2},$$

$$L_{29} = \frac{16ScSrN^3L_{22}}{4N^2 - N_2^2} - \frac{ScSrL_{27}}{4N^2 - N_2^2},$$

$$L_{30} = -\frac{16ScSrN^2L_{21}}{16N^2 - N_2^2}, L_{31} = -\frac{4ScSrN^2L_{22}}{4N^2 - N_2^2},$$

$$L_{32} = \frac{2L_{33}ScSr}{N_2^2}, L_{33} = 2NL_{29} + L_{31},$$

$$C_4 = -\frac{1}{\sinh(N_2\eta) + \beta_3 N_2\cosh(N_2\eta)}\left(\begin{array}{l} L_{28}\sinh(2N\eta) + \\ 2NL_{28}\beta_3\cosh(2N\eta) \end{array}\right)$$

References

[1] T. W. Latham, "Fluid motion in a peristaltic pump", *MS. Thesis, Massachusetts Institute of Technology, Cambridge*, (1966).

[2] A. H. Shapiro, M. Y. Jaffrin, and S. L. Weinberg, "Peristaltic pumping with long wave lengths at low Reynolds numbers", *Journal of Fluid Mechanics*, Vol. 37, No. 4, pp. 799-825, (1969).

[3] H. L. Agrawal, and B. Anwaruddin, "Peristaltic flow of blood in a branch", *Ranchi University Mathematical Journal*, Vol. 15, pp. 111-125, (1984).

[4] L. M. Srivastava, and V. P. Srivastava, "Peristaltic transport of a power-law fluid: Application to the ductus efferentes of the reproductive tract", *Rheologica Acta* , Vol. 27, No. 4, pp. 428-433, (1988).

[5] M. Mishra, and A. R. Rao," Peristaltic transport of a Newtonian fluid in an asymmetric channel", *Zeitschrift für angewandte Mathematik und Physik ZAMP*, Vol. 54, No. 3, pp. 532-550, (2003).

[6] Kh. S. Mekheimer, and Y. Abd elmaboud, "Peristaltic flow through a porous medium in an annulus": Application of an endoscope, *Applied Mathematics & Information Sciences*, Vol. 2 , No. 1, pp. 103-111, (2008).

[7] R. E. Powell, and H. Eyring, "Mechanisms for the relaxation theory of viscosity", *Nature*,Vol. 154, No. 3909, pp. 427-428, (1944).

[8] H. K. Yoon, and A. J. OhaJar, "A note on the Powell Eyring fluid model", *International Communicationsin Heat Mass transfer*, Vol. 14, No. 4, pp. 381-390, (1987).

[9] N. S. Akbar, and S. Nadeem, "Characteristics of heating scheme and mass transfer on the peristaltic flow for an Eyring–Powell fluid in an endoscope", *International Journal of Heat Mass Transf*er, Vol. 55, pp. 375-383, (2012).

[10]T. Hayat, S. I. Shah, B. Ahmad, M. Mustafa," Effect of slip on peristaltic flow of Powell–Eyring fluid in asymmetric channel", *Applied Bionics and Biomechanics.*, Vol. 11, No. 1-2, pp. 69-79, (2014).

[11]N. T. M. Eldabe, M. F. El-Sayed, A. Y. Ghaly, and H. M. Sayed, "Mixed convective heat and mass transfer in a non-Newtonian fluid at a peristaltic surface with temperature-dependent viscosity", *Archive of Applied Mechanics*, Vol. 78, pp. 599-624,(2008).

[12] S. Srinivas, and M. Kothandapani, "The influence of heat and mass transfer on MHD peristaltic flow through a porous space with compliant walls", *Applied Mathematics and Computation*, Vol. 213, No. 1, pp. 197-208 (2009).

[13] S. Srinivas, and M. Kothandapani, "Peristaltic transport in an asymmetric

channel with heat transfer—a note", International Communications in Heat and Mass Transfer, Vol. 35, No. 4, pp. 514-522, (2008).

[14] T. A. Ogulu, "Effect of heat generation on low Reynolds number fluid and mass transport in a single lymphatic blood vessel with uniform magnetic field", *International Communications in Heat and Mass Transfer* , Vol. 33, No. 6, pp. 790-799, (2006).

[15] M. Gnaneswara Reddy, and K. Venugopal Reddy," Influence of Joule heating on MHD peristaltic flow of a Nanofluid with compliant walls", *Procedia Engineering* Vol. 127, pp. 1002-1009, (2015).

[16] M. Gnaneswara Reddy and K. Venugopal Reddy, "Impact of velocity slip and joule heating on MHD peristaltic flow through a porous medium with chemical reaction", *Journal of the Nigerian Mathematical society*, Vol. 35, No. 4, pp. 227-244, (2016).

[17] S. Hina, "MHD peristaltic transport of Eyring-Powell fluid with heat and mass transfer, wall properties and slip conditions", *Journal of Magnetism and Magnetic Materials*, Vol. 404, pp. 148-158, (2016).

[18] M. Gnaneswara Reddy, K. Venugopal Reddy, and O.D. Makinde, "Hydromagnetic peristaltic motion of a reacting and radiating couple Stress fluid in an inclined asymmetric channel filled with a porous medium"**,** *Alexandria Engineering Journal*, Vol. 55, No. 2, pp. 1841-1853, (2016).

How to cite this paper:

K. Venugopal Reddy and M. Gnaneswara Reddy*,"* MHD thermal radiation and chemical reaction effects with peristaltic transport of the Eyring-Powell fluid through a porous medium" *Journal of Computational and Applied Research in Mechanical Engineering*, Vol. 9, No. 1, pp. 85-101, (2019).

DOI: 10.22061/jcarme.2018.2840.1293

URL: http://jcarme.sru.ac.ir/?_action=showPDF&article=952